JOURNAL OF QUATERNARY SCIENCE (2017) **32**(1) 48–62 ISSN 0267-8179. DOI: 10.1002/jqs.2922

JQS Journal of Quaternary Science QRA Quaternary Research Association

New age constraints for the limit of the British–Irish Ice Sheet on the Isles of Scilly

R. K. SMEDLEY,[1]* J. D. SCOURSE,[2] D. SMALL,[3] J. F. HIEMSTRA,[4] G. A. T. DULLER,[1] M. D. BATEMAN,[5] M. J. BURKE,[6] R. C. CHIVERRELL,[6] C. D. CLARK,[5] S. M. DAVIES,[4] D. FABEL,[7] D. M. GHEORGHIU,[8] D. MCCARROLL,[4] A. MEDIALDEA[5] and S. XU[7]

[1]Department of Geography and Earth Sciences, Aberystwyth University, Ceredigion, UK
[2]School of Ocean Sciences, Bangor University, Menai Bridge, Anglesey, UK
[3]School of Geographical and Earth Sciences, University of Glasgow, UK
[4]Department of Geography, Swansea University, Singleton Park, Swansea, UK
[5]Department of Geography, University of Sheffield, UK
[6]School of Environmental Sciences, University of Liverpool, Liverpool, UK
[7]Scottish Universities Environmental Research Centre, East Kilbride, UK
[8]NERC Cosmogenic Isotope Analysis Facility, Scottish Enterprise Technology Park, East Kilbride, UK

Received 16 June 2016; Revised 11 October 2016; Accepted 4 November 2016

ABSTRACT: The southernmost terrestrial extent of the Irish Sea Ice Stream (ISIS), which drained a large proportion of the last British–Irish Ice Sheet, impinged on to the Isles of Scilly during Marine Isotope Stage 2. However, the age of this ice limit has been contested and the interpretation that this occurred during the Last Glacial Maximum (LGM) remains controversial. This study reports new ages using optically stimulated luminescence (OSL) dating of outwash sediments at Battery, Tresco (25.5 ± 1.5 ka), and terrestrial cosmogenic nuclide exposure dating of boulders overlying till on Scilly Rock (25.9 ± 1.6 ka), which confirm that the ISIS reached the Isles of Scilly during the LGM. The ages demonstrate this ice advance on to the northern Isles of Scilly occurred at ~26 ka around the time of increased ice-rafted debris in the adjacent marine record from the continental margin, which coincided with Heinrich Event 2 at ~24 ka. OSL dating (19.6 ± 1.5 ka) of the post-glacial Hell Bay Gravel at Battery suggests there was then an ~5-ka delay between primary deposition and aeolian reworking of the glacigenic sediment, during a time when the ISIS ice front was oscillating on and around the Llŷn Peninsula, ~390 km to the north.

KEYWORDS: British–Irish Ice Sheet; ice stream; Last Glacial Maximum; OSL; TCN.

Introduction

Providing accurate age constraints for the behaviour of palaeo-ice sheets is important for testing ice-sheet models (e.g. Stokes *et al.*, 2015). BRITICE-CHRONO is a large consortium project that is generating an extensive dataset constraining the retreat of the last British–Irish Ice Sheet (BIIS) from its maximum extent during Marine Isotope Stage (MIS) 2. Determining accurate ages for the proposed glacial limit on the Isles of Scilly (Scourse, 1991) is important for reconstructing ice retreat as this is the southernmost terrestrial record of a possible short-lived advance of the Irish Sea Ice Stream (ISIS) into the central Celtic Sea, previously described as a surge (Scourse *et al.*, 1990; Scourse and Furze, 2001; Chiverrell *et al.*, 2013). Despite some views to the contrary (Coque-Delhuille and Veyret, 1984, 1989), there has been a *consensus* over the position of an ice limit (Fig. 1) on the Isles of Scilly (Barrow, 1906; Mitchell and Orme, 1967; Scourse, 1991) following the first identification of erratic material in the 19th century (Smith, 1858). The age of this ice limit has, however, been contested and the interpretation that this occurred during MIS 2 remains controversial (cf. McCabe, 2008). Mitchell and Orme (1967) and Bowen (1973) argued that the glacial deposits were of Wolstonian age (MIS 6) on the basis of lithostratigraphic correlation with coastal sequences elsewhere around the Irish Sea Basin; this was later revised by Bowen (1999) to MIS 16. However, Scourse (1991) has interpreted the glacigenic sediment-landform suite to be of Late Devensian (MIS 2) age on the basis of geochronological data.

Published radiocarbon, thermoluminescence (TL), optically stimulated luminescence (OSL) and terrestrial cosmogenic nuclide (TCN) ages for the most recent advance of ice on to the Isles of Scilly indicate an age within the Last Glacial maximum (LGM) (Clark *et al.*, 2009). However, the spread in these ages is large and it is difficult to determine whether any readvance may have been involved. Bayesian analysis of the existing geochronological (^{14}C, OSL, TCN) data combined with the prior knowledge of ice retreat for the entire ISIS have been used to reduce the uncertainties inherent to the individual techniques, and model ice impingement on to the Isles of Scilly at 23.3–24.0 ka (Chiverrell *et al.*, 2013). The timing of this advance was accompanied by an associated increase in ISIS-sourced ice-rafted detritus (IRD) flux to the adjacent deep ocean (Scourse *et al.*, 2009a) and agrees with recent ^{14}C dating of an arctic bivalve recovered from glacigenic sediments cored close to the shelf break in the Irish sector of the Celtic Sea (Praeg *et al.*, 2015).

The age and extent of the glacial evidence on Scilly has implications for the glaciation of the wider Celtic Sea and for the wider dynamics of the BIIS. While the *consensus* of an ice limit on Scilly might imply that this marks the maximum extent of glaciation, Scourse *et al.* (1990) documented evidence for grounded ice and, to the south-west, glacimarine conditions (Melville Till and Melville Laminated Clay) into the central Celtic Sea. This has been considered the maximum extent of ice advance across the Celtic shelf, but the recent evidence reported by Praeg *et al.* (2015) places the

*Correspondence to: R. K. Smedley, as above.
E-mail: rks09@aber.ac.uk

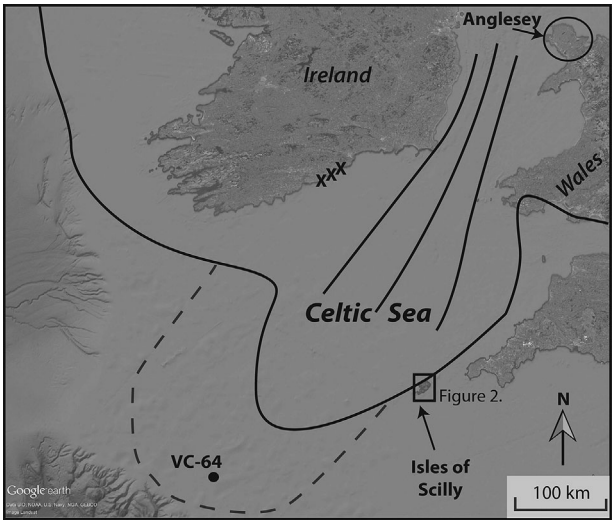

Figure 1. Google Earth image of the Isles of Scilly showing the Irish Sea Ice Stream within the wider context of the Celtic Sea. Solid line is the ice limit after Scourse *et al.* (1990), and dashed line is an inferred limit based on the interpretation that the ISIS reached the shelf edge (Praeg *et al.*, 2015). The core site (VC-64) on which this interpretation is based is also shown. Flow lines of the ISIS adapted from Chiverrell *et al.* (2013). Black crosses mark dated sites in southern Ireland (Cofaigh and Evans, 2007; Cofaigh *et al.*, 2012). Place names mentioned in the text are shown.

Scilly ice limit in a new context (Fig. 1); does it represent a lateral ice limit to the ISIS, flowing southwards from the north to the west, or does it represent a terminal limit to a larger ice body on the Irish shelf to the west with driving stresses from the north-west? Certainly, the ice flow data and the distribution of glacigenic sediment units on Scilly (Hiemstra *et al.*, 2006) are consistent with ice flow from the north-west rather than from the north.

Although previous studies have provided ^{14}C, TL, OSL and TCN ages for the presence of ice on the Isles of Scilly, the reliability of some of the ages is questioned (see Supporting Information, Table S1 for details). Conventional radiocarbon ages on humic-humin fractions of tundra pollen-bearing organic sequences lying stratigraphically below the glacigenic sequence from multiple sites (Scourse, 1991) yielded finite ages between 39.0 ± 2.1 and 23.9 ± 1.8 ka BP for samples Q-2446 and Q-2358/9, respectively, when re-calibrated using IntCal13 (Reimer *et al.*, 2013). However, the accuracy of these ages was potentially compromised by contamination with younger carbon derived from burrowing bees, rootlet and groundwater sources because the sampled organic sequences were in open coastal sections. The reliability of the existing TL and OSL data from the Isles of Scilly is also questioned as either the data were determined using experimental methods (Wintle, 1981; Smith *et al.*, 1990) or the publications lacked sufficient detail about the analyses, such as dose-recovery experiments (Evans *et al.*, 2006a; Scourse and Rhodes, 2006). Finally, an assessment of radionuclide inheritance cannot be made for the TCN age from Shipman Head (McCarroll *et al.*, 2010) as it was determined from a single boulder (see section 'Shipman Head, Bryher').

As a consequence, a recent review of legacy geochronological data relating to the reconstruction of the BIIS by the BRITICE-CHRONO Consortium Project (Small *et al.*, in press) considered the existing chronology for the Isles of Scilly determined from ^{14}C, TL, OSL and TCN dating not to be reliable for constraining ice retreat. Therefore, the aim of this paper is to report new geochronological (OSL, TCN) data for the ice advance to the Isles of Scilly. Improving the age constraints on ice advance to the Isles of Scilly is important as it will develop our understanding of changes in ice sheet dynamics relative to the IRD flux in the adjacent marine record.

Study sites and sample descriptions

A significant ice limit across the northern Isles of Scilly is delineated by boulders, glacigenic sedimentary units and associated landform elements (Fig. 2). The lithostratigraphical relationship between the sedimentary units (Fig. 2) has previously been established by Scourse (1991). An advance of the ISIS is indicated by an ice-marginal diamicton at Bread and Cheese Cove, St Martin's, defined as the Scilly Till (Scourse, 1991) and suggested to have been subglacially emplaced and post-depositionally glacitectonized (Hiemstra *et al.*, 2006). At this site, the ISIS advanced over pre-existing marine and contemporaneous proglacial lacustrine sediments in a similar fashion to that proposed by Ó Cofaigh and Evans (2001a,b) and Evans and Ó Cofaigh (2003) for Irish Sea Till deposition in south-east Ireland. The Scilly Till (Scourse, 1991) also forms the core of a series of major inter-tidal bars in the northern Isles of Scilly (White Island, Bar, Pernagie Bar and possibly also Golden Ball Brow; Fig. 2) interpreted as latero-frontal moraine loops demarcating the onshore flow of lobate ice sheet margins (Scourse, 1991; Scourse and Furze, 2001; Hiemstra *et al.*, 2006).

Battery and Gunhill, Tresco

The coastal section at Battery, Tresco (49°58′N, 6°20′W) (Fig. 2) is described in Scourse (1991). Ice-proximal outwash sands and gravels (Tregarthen Gravel) at this site are similar to outwash deposits found at Bread and Cheese Cove, St Martin's, in association with the stratotype of the Scilly Till (Scourse, 1991). OSL ages have previously been determined for sedimentary units at both sites (Scourse *et al.*, 2004; Evans *et al.*, 2006a; Scourse and Rhodes, 2006), but are regarded as preliminary because full details of the samples and techniques are not provided (Table S1). Results from Bread and Cheese Cove suggest that the Scilly Till developed glacitectonic structures after 49 ± 3 ka, producing a till largely derived from sediments deposited during MIS 5 (Evans *et al.*, 2006a).

Four deglacial, ice-proximal, lenses consisting of well-sorted sands containing rounded to sub-rounded erratic clasts represent the Tregarthen Gravel at Battery, and are interbedded with gelifluctates correlated with the Bread and Cheese Breccia (Fig. 3); this sequence is described and interpreted in Scourse (1991). The gelifluctates sampled for OSL dating represent sediment flows down the slopes of the valley transverse to the palaeocurrent direction. The erratic clasts within the sand lenses form gravel lags at the base, with the palaeocurrent direction inferred to have been from west to east. Four sedimentary samples (T4BATT01, T4BATT03, T4BATT04 and T4BATT05) were taken from the Tregarthen Gravel at Battery for OSL dating (Fig. 3). Sample T4BATT01 was taken from horizontally laminated medium-to-coarse sand at a depth of 3 m. Sample T4BATT03 was taken at a depth of 1.8 m, from a 0.4-m-thick channel-fill unit composed of planar cross-set, fine-to-medium sand and granular gravel. Sample T4BATT04 was taken from the section at a depth of 2.8 m and is composed of horizontally stratified, fine-to-medium sand. Finally, sample T4BATT05 was the lowest sample taken, at a depth of 2.5 m, from horizontally stratified medium sand and some granular gravel.

A fifth OSL sample (T4BATT06) was taken at Battery from a depth of 1 m within a unit of horizontally stratified silt-to-medium sand (Fig. 3) comprising the post-glacial Hell Bay Gravel that caps the Tregarthen Gravel (Fig. 2). The Hell

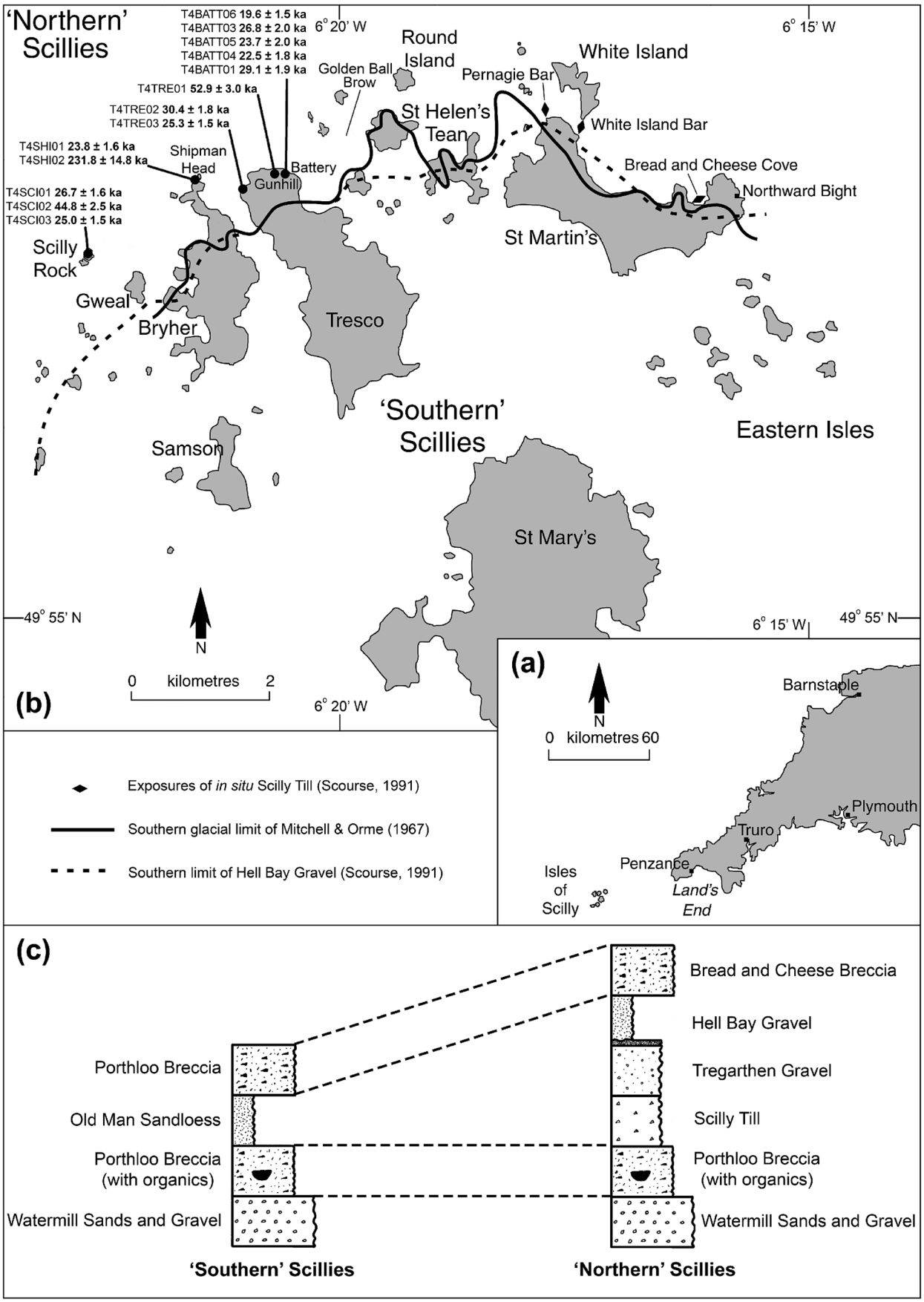

Figure 2. Location of the Isles of Scilly in south-west Britain (a). The northern Isles of Scilly with the sites and associated dates discussed in the text where the inferred maximum ice limit is also shown (b). The lithostratigraphic models for the southern and northern Isles of Scilly (c; Scourse, 1991; Scourse and Furze, 2001; Scourse *et al.*, 2009a). The Scilly Till and Tregarthen Gravel represent primary *in situ* glacigenic units. The Hell Bay Gravel represents a soliflucted admixture of Old Man Sandloess, Tregarthen Gravel and Scilly Till. The Bread and Cheese Breccia and upper Porthloo Breccia represent a final phase of solifluction.

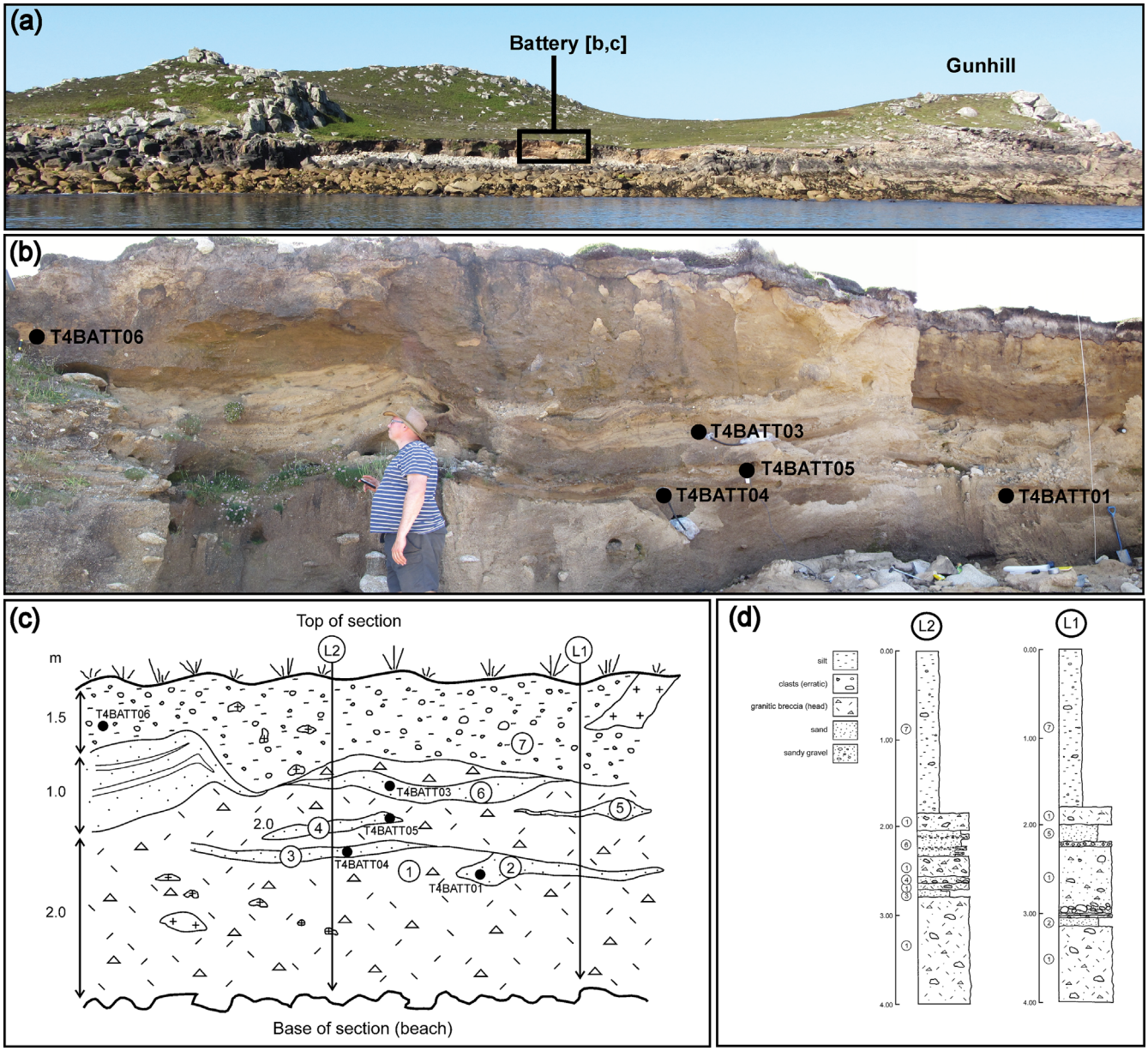

Figure 3. Battery and Gunhill sites on the Isles of Scilly (a) and the sedimentary section at Battery shown as a photograph (b) and interpretation (c), including the sedimentary logs (d). Also shown are the five samples taken for OSL dating (samples T4BATT01, T4BATT03, T4BATT04, T4BATT05 and T4BATT06).

Bay Gravel is interpreted as gelifluctates derived from the glacigenic units (Scilly Till, Tregarthen Gravel) deposited penecontemporaneously with widespread sandloess (Old Man Sandloess) associated with the Scilly Till. Scourse (1991) has interpreted the Old Man Sandloess as genetically associated with the glacial event. Two TL ages both of 18.6 ± 3.7 ka (Wintle, 1981) and an OSL age of 20 ± 7 ka (Smith *et al.*, 1990)[1] have previously been published for the deposition of the Old Man Sandloess.

On Gunhill, and northern Tresco in general, there are a number of isolated boulders, and some erratic clasts at the surface (Fig. 3a); two boulders and one erratic clast were sampled for TCN dating. Sample T4TRE01 was taken from a granite boulder proximal to a tor displaying some signs of glacial modification (cf. McCarroll *et al.*, 2010). Sample T4TRE02 was collected from a large tabular granite boulder that has been moved *ca.* 50 m from its parent tor. The upper surface of this boulder displays no weathering pits or runnels, suggesting that it has either been overturned or had overlying material removed. Given the flat nature of the top surface, it is likely that separation occurred along a pre-existing joint within the granite bedrock. The sampled boulder occurs at the same altitude as the parent tor; thus, it is unlikely that periglacial processes, such as boulder ploughing (Ballantyne, 2001), could have separated the boulder from its parent tor, overturned it and moved it to its present position. This boulder occurs at an elevation of ~32 m OD which is within the limit of storm waves on Scilly (see discussion of Scilly Rock below) but is shielded from wave activity by the higher ridge forming the northern coast of Tresco. The site is now fully vegetated, whereas storm-influenced contexts are devoid of soil and vegetation. Given this geomorphological context, it is likely that the only mechanism that could have been responsible for boulder mobilization is ice. Sample T4TRE03 was obtained from a cobble clast sampled from the surface and within the maximum extent of glacial deposits (Scourse, 1991). The cobble was a grey, coarse-grained, non-foliated rock composed of >90% quartz. No sedimentary structures

[1]An age for sample 741al was reported in Scourse (1991) however, this sample does not feature in the original publication by Smith *et al.* (1990) and so cannot be included here.

were visible and during crushing the rock fractured through the quartz crystals. It is thus identified as a quartzite and bears affinity to the Holyhead quartzite (Phillips, 1991) and bedrock found in eastern Ireland (Brück and Reeves, 1976). The Isles of Scilly are composed entirely of Variscan granite of the Cornubian batholith; therefore, the clast is interpreted as an erratic probably from exposures on the east coast of Ireland and on Anglesey in Wales within the trunk of the ISIS. A full description of the lithologies and likely bedrock sources of erratics from the Isles of Scilly is included as *Appendix* 2 in Scourse (1991).

Shipman Head, Bryher

A linear collection of free-standing boulders positioned just inside the ice limit on Shipman Head (49°57′N, 6°21′W), Bryher, has been interpreted as a 'boulder moraine' (McCarroll *et al.*, 2010). The limit is further marked by a change in the character of granite tors from heavily eroded forms north of the ice limit to highly ornate castellated or mammilated forms with abundant free-standing core-stones south of the limit (Scourse, 1991; Hiemstra *et al.*, 2006). TCN dating has previously generated a ^{10}Be age of 20.9 ± 2.2 ka (McCarroll *et al.*, 2010), recalculated to 22.1 ± 1.3 ka using a production rate derived at Loch Lomond (Fabel *et al.*, 2012) for the upper surface of an ~27-m^3 granite boulder that is 3 m high, measured from the highly weathered underside to the sampled top surface. This boulder was interpreted to have been mobilized by ice from a nearby tor and subsequently inverted as the underside contains a network of weathering pits and drainage channels. However, these features also imply significant exposure before overturning. Such an extended period is also suggested by exposure ages of 95.3 ± 5.2 and 143.9 ± 8.7 ka from granite tors outside the maximum extent of glaciation (McCarroll *et al.*, 2010). This raises the possibility that the apparent exposure age may be overestimated as it contains a significant contribution of ^{10}Be from deeply penetrating muons (cf. Braucher *et al.*, 2003). To test this hypothesis, a sample was collected from the top (T4SHI01) and bottom (T4SHI02) weathered surfaces of the boulder reported in McCarroll *et al.* (2010; Fig. 2 in which full site details and context are provided).

Scilly Rock

Scilly Rock (49°57′N, 6°22′W) is a small granite island (0.25 km by 0.12 km) on the north-west extremity of the Scilly archipelago, situated 1.50 km west of Bryher and 0.75 km north-west of the island of Gweal (Fig. 2). Scilly Rock was not surveyed by Scourse (1991) nor, to our knowledge, visited by Mitchell and Orme during their work in the 1960s. However, the latter authors comment that 'The rocks to the west of Bryher and Gweal have been largely washed clean of superficial material. Scilly Rock, to the north-west, has traces of superficial material (head?) in some fissures, and the profile of the Rock suggests that it has been smoothed by ice' (Mitchell and Orme, 1967, p. 78). Following observation from a small boat of a prominent linear ridge of loose boulders, fieldwork was undertaken by the authors during the summer of 2013 and is the first report of the Pleistocene sequence and landforms of the island.

Scilly Rock is heavily fissured and rugged, reaching a maximum elevation of ~22 m along the central spine of the island which trends NE–SW, but the fissures that follow a structural lineation in the granite trend NW–SE and create a series of deep gullies, some of which extend to below sea level (Fig. 4a). One particularly prominent gully divides Scilly Rock almost in two, a deep fissure separating the south-west part of the island from the rest (Fig. 4a). It was not possible to land on this south-western part of the island, so all the observations below relate to the larger north-eastern portion. The linear boulder feature is located along the central spine of the island at its highest elevation. The boulders forming this feature are all granite and vary in size from cobbles to >10 m^3. Many of the boulders rest on the solid granite without any matrix present, but some rest on a diamicton matrix consisting of very poorly sorted silty sand with some clay containing abundant erratic clasts. This diamicton was sampled for micromorphological analyses to determine the depositional context of this sediment. Although no large erratics were observed, the lithic assemblage of smaller clasts was identical to that found in the Hell Bay Gravel, Scilly Till and Tregarthen Gravel, which are notably rich in Cretaceous flint, and red and grey sandstones (Scourse, 1991). Also, some of the clasts are clearly faceted and striated. This material is currently being actively eroded by storm waves, which have been observed to break over the summit of the island (Fig. 4b), so only fragments remain in the more protected situations under large boulders. The preliminary field interpretation of the Scilly Rock boulder accumulation was that it was glacial in origin, so a number of the boulders that were deposited on the potential glacial material (e.g. Fig. 4c) were sampled for TCN analysis (T4SCI01, T4SCI02 and T4SCI03).

Methods

OSL dating

All five samples for OSL dating were collected in opaque tubes that were hammered into the sedimentary section to prevent exposure to sunlight during sample collection. External beta dose-rates were determined for OSL dating using inductively coupled plasma mass spectrometry (ICP-MS) and inductively coupled plasma atomic emission spectroscopy (ICP-AES), while the external gamma dose-rates were determined using *in situ* gamma spectrometry (Table 1). The external beta dose-rates were also determined using a Risø GM-25-5 beta counter to assess the accuracy of these measurements; the results were within uncertainties of the beta dose-rates determined using the ICP analyses. In addition, the external gamma dose-rates were calculated using the chemical concentrations determined from ICP-MS and compared with the gamma dose-rates determined using *in situ* gamma spectrometry. The external gamma dose-rates for sample T4BATT06 were similar when determined using the field gamma spectrometry (1.14 ± 0.07 Gy ka^{-1}) and ICP-MS results (1.08 ± 0.08 Gy ka^{-1}). Sample T4BATT06 was taken from a thick sedimentary unit >0.3 m away from any boundaries and so the ICP-MS results provided an accurate estimate of the gamma dose-rate that was similar to the dose-rate determined using *in situ* gamma spectrometry. However, the external gamma dose-rates determined using field gamma spectrometry for the four samples taken from the Tregarthen Gravel were 0.9 Gy ka^{-1} (T4BATT01), 0.3 Gy ka^{-1} (T4BATT03), 0.7 Gy ka^{-1} (T4BATT04) and 0.6 Gy ka^{-1} (T4BATT05) higher than those determined using the ICP results; this is calculated relative to the central value of the gamma dose-rate and excluding uncertainties, which are typically 10–15% of the gamma dose-rate. The differences for the four samples from the Tregarthen Gravel are probably because these samples were taken from units that were thinner than the effective range of gamma rays (~0.3 m), and so field gamma spectrometry was required to accurately determine the external gamma dose-rate *in situ*. Given the challenging nature of the thin sand lenses sampled from the

Figure 4. Photographs of Scilly Rock and the gully that divides the island (a). Waves breaking over the summit of Round Island, 6 km north-west of Scilly Rock (10 March 2008) demonstrating the likelihood of storm activity in removing superficial sediments from these exposed settings (b). Round Island summit is 35 m above Ordnance Datum (OD) and Scilly Rock is 22 m above OD (photos: Dave Mawer). Photograph of a boulder sampled for TCN dating (sample T4SCI01) resting on sediment sampled for micromorphological analysis (c).

Tregarthen Gravel, four replicate samples were taken for OSL dating from this unit to constrain the depositional event.

To isolate coarse-grained quartz for OSL analysis, each sample was first treated with a 10% v/v dilution of 37% HCl and with 20% v/v of H_2O_2 to remove carbonates and organics, respectively. Dry sieving isolated the 212–250 μm diameter grains, and density-separation using sodium polytungstate provided the 2.62–2.70 g cm^{-3} (quartz-dominated) fractions. The quartz grains were etched for 1 h in 40% hydrofluoric (HF) acid to remove the outer portion of the quartz grains affected by alpha irradiation and to remove any contaminating grains of feldspar. After the etching, the quartz was washed in 10% HCl to remove any fluorides that may have been produced during HF etching and re-sieved at 212 μm. Grains were mounted into 10 by 10 grids of 300-μm-diameter holes in a 9.8-mm-diameter aluminium single-grain disc for analysis.

All luminescence measurements were performed using a Risø TL/OSL DA-15 automated single-grain system equipped with a ^{90}Sr/^{90}Y beta source (Bøtter-Jensen *et al.*, 2003). Stimulation was performed using a green laser and detected through a 2.5-mm-thick U-340 filter and convex quartz lens placed in front of the photomultiplier tube. The signal was recorded at 125 °C for a total of 1 s, where the OSL signal was summed over the first 0.1 s of stimulation and the background calculated from the final 0.2 s. Instrument reproducibility of 2.5% (Thomsen *et al.*, 2005) was incorporated into the calculation of the equivalent dose (D_e) values. The preheat temperature was determined from a dose-recovery preheat plateau test performed on multiple-grain aliquots (5 mm in diameter) of sample T4BATT03. The results suggested that the D_e values determined were not dependent upon the preheat temperature used, but recuperation was >5% above preheat temperatures of 220 °C. Therefore, a preheat of 220 °C for 10 s and cutheat of 160 °C were used for the single aliquot regenerative dose (SAR) protocol (Murray and Wintle, 2000). Dose-recovery experiments performed suggested that the SAR protocol was appropriate for OSL dating: T4BATT03 (ratio of 0.94 ± 0.02, overdispersion = 5 ± 1%); T4BATT04 (ratio of 0.95 ± 0.04, overdispersion = 15 ± 1%) and T4BATT06 (ratio of 0.98 ± 0.03, overdispersion = 7 ± 1%).

Six screening criteria were applied to the data throughout the analyses; associated uncertainties were included for each test. Grains were only accepted if the response to the test dose was greater than three sigma above the background, the test dose uncertainty was <20%, the recycling ratios and OSL-IR depletion ratios were within the range 0.8–1.2, recuperation was <5% of the response from the largest regenerative dose (150 Gy) and the single-grain D_e values were not part of a population of very low doses that were identified by the finite mixture model (FMM) to be inconsistent with the geological context of the sample (i.e. ≤1 ka). Only 0–8% of grains giving a D_e value failed this last criterion. After applying all screening criteria, between 2.6 and 3.9% of the total grains analysed were used to calculate D_e values that were then used for age calculation (Table 1).

TCN dating

Eight samples from three locations inferred to be within the maximum extent of the ISIS were collected for analysis of *in situ* produced ^{10}Be in quartz (Table 2). Shielding from surrounding topography was measured and corrected for using the CRONUS-Earth online calculator (Table 2; Balco *et al.*, 2008). The boulder samples were chiselled from upper boulder surfaces and the cobble sample (T4TRE03) was collected as a whole clast.

Samples were crushed and washed at the University of Glasgow. Quartz was separated from the 250–500 μm fraction using standard mineral separation techniques and purified by ultrasonication in 2% HF/HNO_3 to remove remaining contaminants and meteoric ^{10}Be. Quartz purity was assessed by measuring the aluminium content using flame atomic absorption spectrometry. Beryllium extraction was carried out at the Cosmogenic Isotope Analysis Facility – Scottish Universities Environmental Research Centre (CIAF – SUERC), using procedures based on Child *et al.* (2000). The ^{10}Be/^{9}Be ratios were measured by accelerator mass spectrometry (AMS) at SUERC (Xu *et al.*, 2010) and ^{10}Be exposure ages were calculated using the CRONUS-Earth online calculator (Table 2; Balco *et al.*, 2008). See Table S2 for details on the chemistry and AMS data for these analyses. Exposure ages presented are based on the time-dependent Lm scaling (Lal, 1991; Stone, 2000) and assuming an erosion rate of 1 mm ka^{-1}. Assuming an erosion rate of 0 mm ka^{-1} would change our ages by <3% and not impact upon any conclusions of this study (Table 2).

Table 1. Concentrations of K, Rb, U and Th determined for OSL dating using ICP-MS and ICP-AES analysis, presented to the appropriate decimal places according to the associated detection limits. The beta dose-rates were calculated using the conversion factors of Guerin *et al.* (2011) and beta dose-rate attenuation factors of Guérin *et al.* (2012). Gamma dose-rates were measured *in situ* using a portable gamma spectrometer. Water contents of 17 ± 5% were applied and are expressed as a percentage of the mass of dry sediment. The water contents were estimated from the field and saturated water contents, and environmental history for each sample. Cosmic dose-rates were determined in accordance with Prescott and Hutton (1994). Dose-rates were calculated using the Dose Rate and Age Calculator (DRAC; Durcan *et al.*, 2015). Note that the full sample codes include a prefix of Aber209/.

Sample	Depth (m)	K (%)	Rb (ppm)	U (ppm)	Th (ppm)	Beta dose-rate (Gy ka^{-1})	Gamma dose-rate (Gy ka^{-1})	Cosmic dose-rate (Gy ka^{-1})	Total dose-rate (Gy ka^{-1})	No. of grains measured (and accepted for D_e)	D_e (Gy)	Age (ka)
T4BATT01	3.3	0.7 ± 0.1	43.4 ± 4.3	1.82 ± 0.18	7.0 ± 0.7	0.71 ± 0.06	1.48 ± 0.10	0.13 ± 0.01	2.35 ± 0.12	2700 (106)	68.5 ± 2.8	29.1 ± 1.9
T4BATT03	1.8	0.9 ± 0.1	54.8 ± 5.5	2.40 ± 0.24	5.7 ± 0.6	0.87 ± 0.08	0.95 ± 0.06	0.16 ± 0.02	2.01 ± 0.10	2600 (67)	53.8 ± 2.9	26.8 ± 2.0
T4BATT04	2.8	1.4 ± 0.1	96.9 ± 9.7	1.70 ± 0.17	5.0 ± 0.5	1.09 ± 0.10	1.40 ± 0.10	0.14 ± 0.01	2.66 ± 0.14	2400 (64)	60.0 ± 3.7	22.5 ± 1.8
T4BATT05	2.3	1.4 ± 0.1	117.7 ± 11.7	1.91 ± 0.19	5.7 ± 0.6	1.13 ± 0.11	1.34 ± 0.09	0.15 ± 0.02	2.65 ± 0.14	1800 (51)	62.7 ± 4.0	23.7 ± 2.0
T4BATT06	1.0	2.0 ± 0.2	124.0 ± 12.4	2.98 ± 0.30	9.5 ± 1.0	1.65 ± 0.15	1.14 ± 0.07	0.18 ± 0.02	3.01 ± 0.17	2200 (74)	59.0 ± 3.0	19.6 ± 1.5

Work from high latitudes in both hemispheres report standardized production rates that are 5–15% higher than the global production rate used in the CRONUS calculator (Balco *et al.*, 2008). The post-2008 production rates reduce scaling uncertainties and improve agreement with independent chronological techniques (Balco *et al.*, 2009; Putnam *et al.*, 2010; Fenton *et al.*, 2011; Kaplan *et al.*, 2011 Goehring *et al.*, 2012a,b; Young *et al.*, 2013). Two independently calibrated local production rates are available from the British Isles: (i) the Loch Lomond production rate (LLPR) (Fabel *et al.*, 2012) and (ii) the Glen Roy production rate (GRPR) (Small and Fabel, 2015). These production rates agree within uncertainties (3.92 ± 0.18 and 4.26 ± 0.21 atoms g^{-1} a^{-1}, respectively). The LLPR is preferred in this study as it is derived from direct age control provided by limiting radiocarbon ages (MacLeod *et al.*, 2011), instead of the assumed ages of tephra within a varve chronology (MacLeod *et al.*, 2015) used to determine the GRPR.

Micromorphology

To provide contextual confirmation of the glacigenic interpretation for the boulders sampled for TCN dating on Scilly Rock, a series of monolith samples from the underlying matrix were taken for micromorphological analysis. The samples were impregnated and thin-sectioned to a final thickness of *ca.* 30 μm following established procedures (see Palmer *et al.*, 2008; Hiemstra, 2013). A transmitted-light petrographic microscope (Leica™ DM EP) was used for the analysis, with magnifications of up to 40 times, in both plane- and cross-polarized light settings. Two of the samples were subsequently analysed using micro-X-ray tomography (μCT, Nikon™ Metrology/X-Tek XTH 225). μCT analysis allows the visualization and reconstruction of 3-D phenomena, notably fracture plane geometry and particle long axis fabric, on the basis of 2-D information (see Tarplee *et al.*, 2011).

Results

Shipman Head, Bryher

The boulder samples from Shipman Head on Bryher were collected to assess the reliability of the exposure age obtained by McCarroll *et al.* (2010). Re-sampling of the top surface of the boulder (T4SHI01) produced an exposure age of 23.8 ± 1.6 ka (Table 2), which agrees with the published TCN age (22.2 ± 1.3 ka). The sample collected from the underside of the boulder (T4SHI02) produced an apparent exposure age of 231.8 ± 14.8 ka. Such a prolonged period of exposure before overturning means that the ^{10}Be inventory measured from the upper surface will include a significant muonic contribution as muons can produce ^{10}Be at depths >3 m (Braucher *et al.*, 2003). A simple model of ^{10}Be concentration with depth assuming a total period of exposure before overturning equivalent to the apparent exposure age of 231 ka and no prior inheritance has been determined following Granger and Smith (2000) (Fig. 5). While this model is a first-order quantification of the inherited ^{10}Be inventory due to muons, it demonstrates that a significant proportion (~20%) of the measured ^{10}Be inventory from the top surface is due to production by muons during exposure before overturning. This level of inheritance would produce an apparent exposure age which overestimates the true age of exposure by ~5 ka, suggesting that overturning occurred between *ca.* 19 and 17 ka based on the ages from the upper surface of the boulder in this study and McCarroll *et al.* (2010). While understanding of muon interaction cross-sections has continued to improve (cf. Phillips *et al.*, 2016), the non-trivial level of inheritance

Table 2. Sample information and exposure ages for TCN samples from the Isles of Scilly. Calculations were performed using the CRONUS-Earth online calculator developmental version; wrapper script 2.2, Main calculator 2.1, constants 2.2.1, muons 1.1.

Sample	Lat.	Long.	Alt. (m)	Thickness (cm)	Shielding*	^{10}Be conc. (at g^{-1})†	^{10}Be conc. ±	1 mm ka^{-1} Exposure age (ka)‡	0 mm ka^{-1} Exposure age (ka)‡
T4SHI01	49.965	−6.360	15	1.3	0.9853	94 100	4366	23.8 ± 1.6 (1.1)	23.3 ± 1.4 (1.1)
T4SHI02	49.965	−6.360	15	1.1	0.9972	745 800	14 872	231.8 ± 14.8 (5.9)	193.0 ± 8.7 (4.0)
T4SCI01	49.957	−6.379	18	1.3	1	106 200	3723	26.7 ± 1.6 (1.0)	26.1 ± 1.4 (0.9)
T4SCI02	49.957	−6.379	18	3	0.9997	171 100	4686	44.8 ± 2.5 (1.3)	43.1 ± 2.0 (1.2)
T4SCI03	49.957	−6.379	15	3.7	0.9986	97 500	3776	25.0 ± 1.5 (1.0)	24.5 ± 1.3 (0.9)
T4TRE01	49.967	−6.345	30	2.5	0.9999	206 100	5527	52.9 ± 3.0 (1.5)	50.7 ± 2.4 (1.4)
T4TRE02	49.965	−6.349	32	2.4	1	121 300	4111	30.4 ± 1.8 (1.1)	29.6 ± 1.5 (1.0)
T4TRE03	49.965	−6.349	20	5.3	1	98 100	3500	25.3 ± 1.5 (0.9)	24.7 ± 1.3 (0.8)

*Calculated using the CRONUS calculator (Balco *et al.*, 2008), available at: hess.ess.washington.edu/math/general/skyline_input.php.
†Be analyses were standardized to NIST27900 with ^{10}Be/^{9}Be taken as 2.79×10^{-11}. A process blank correction of $5.89 \pm 1.04 \times 10^{-15}$ was applied to all samples. Concentrations have been rounded to the nearest 100 atoms.
‡Exposure ages calculated using the CRONUS calculator developmental version; Wrapper script 2.2, Main calculator 2.1, Constants 2.2.1, Muons 1.1; hess.ess.washington.edu/math/al_be_v22/al_be_calibrate_v22.php; accessed 25 November 2015 (Balco *et al.*, 2008), Lm scaling, assuming a density of 2.6 g cm^{-3}. Analytical uncertainties are given in parentheses.

due to such a prolonged period of prior exposure will produce a spurious apparent exposure age for the boulder's top surface regardless of the depth-production model used.

Scilly Rock

Diamicton

Microscopically, the diamicton is characterized as matrix supported, albeit with a variable grain density. It shows an abundance of randomly orientated, elongated, irregularly shaped pores, but there are also sets of planar fractures that display regular, symmetrical geometric patterns (subhorizontal and steeply inclined planes), which was corroborated by μCT analysis (Fig. 6a). Pebbles in the diamicton are granitic, often subangular with irregular outlines, showing evidence of *in situ* weathering (exfoliation, rind formation and biotite alteration). Silt and sand grains in the diamicton are highly variable in terms of shape and roundness, and display strong preferred long-axis orientation (micro-fabric) in places. Locally, lineaments and associated turbate structures can be

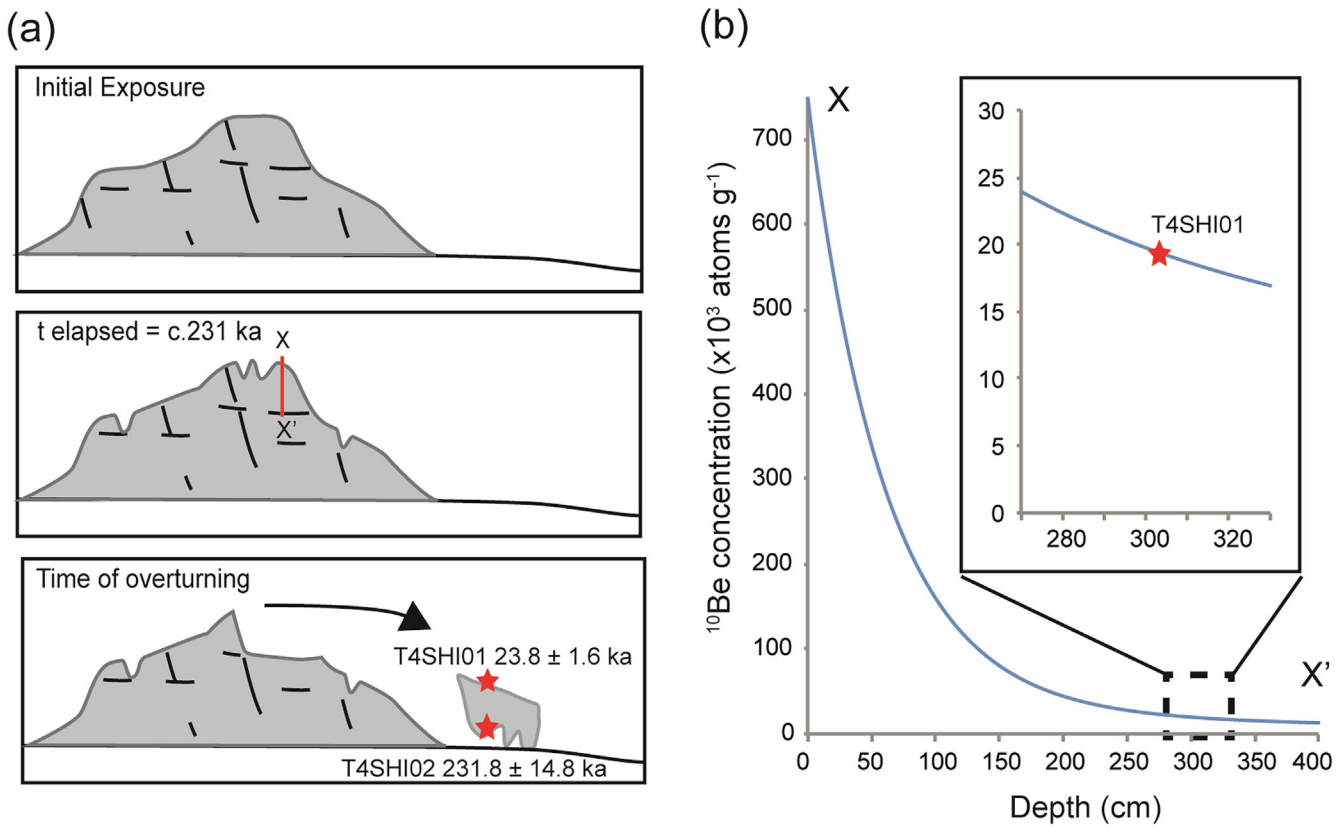

Figure 5. Evolution of the cosmogenic inventory of the Shipman Head boulder. Schematic of the setting at Shipman Head (a). The *in situ* boulder-to-be began accumulating ^{10}Be when initially exposed. This accumulation progressed for *ca.* 231 ka (as indicated by the apparent exposure age of T4SHI02). At the time of overturning a previously shielded surface was exposed from which the original sample of McCarroll *et al.* (2010) and T4SHI01 was collected. Modelled depth profile (X–X′) of ^{10}Be concentration for an exposure period of 231 ka (after Granger and Smith, 2000) (b). The inset panel shows a close-up view of the ^{10}Be accumulated at the depth of the sampled surface (T4SHI01) before overturning. At the time of overturning the ^{10}Be concentration was *ca.* 20 000 atoms g^{-1}.

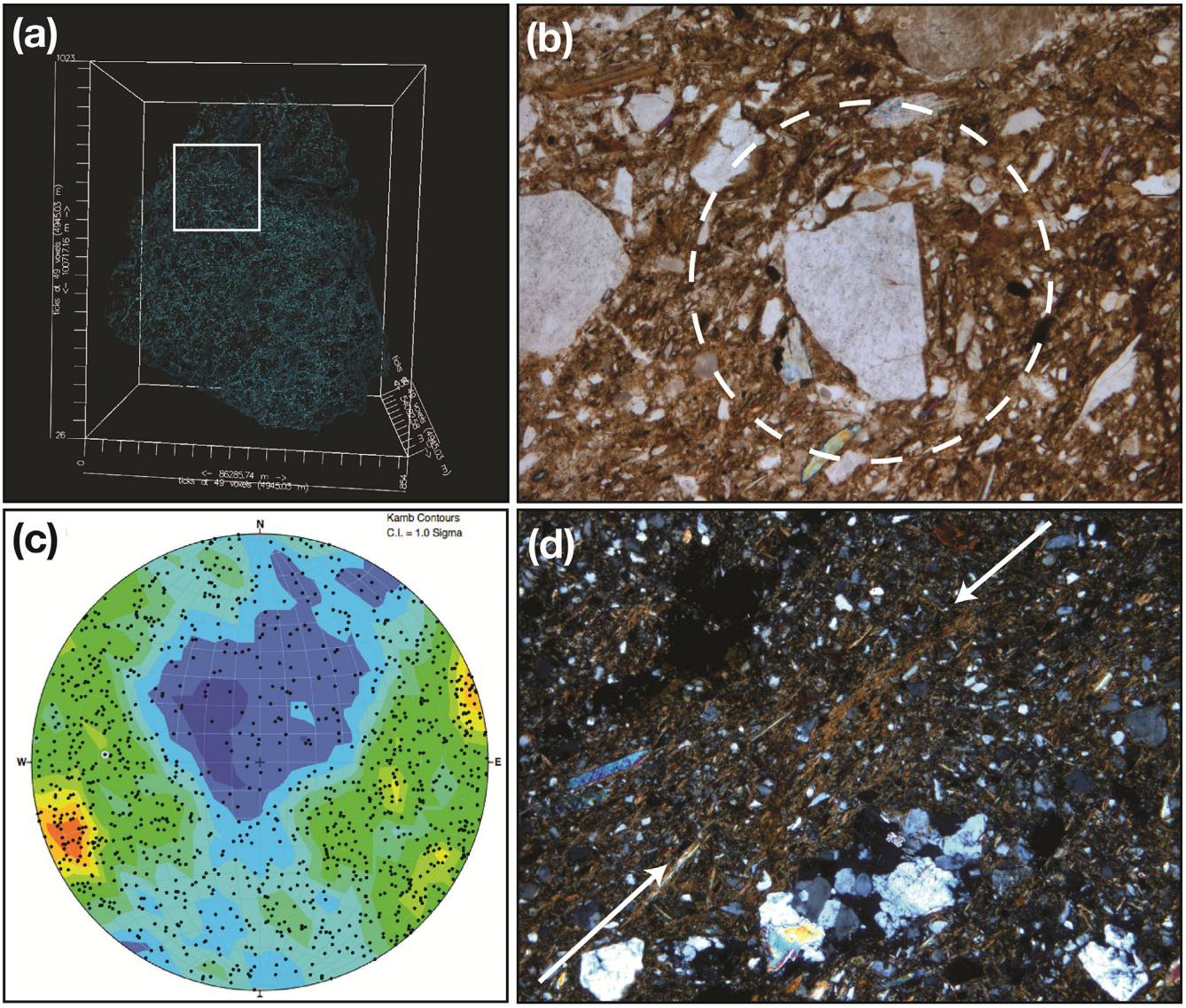

Figure 6. Example of a micro-X-ray tomography image of fracture patterns observed in the Scilly Rock diamicton (a). While the overall appearance of the fracture network is rather chaotic, locally (for example in the white frame indicated) a regular geometric pattern of subhorizontal and steeply inclined planes is visible. Example of turbate microstructure (plane light, width of view 4 mm) defined as circular arrangements of fine elongated grains around a coarse core grain (b). It suggests that the coarse grain rotated in response to simple shear, thereby reorientating the fine-textured material in its direct vicinity. Example of a lower hemisphere equal area stereoplot (with Kamb contouring heat maps) representing silt and sand grain long axis fabric in the Scilly Rock diamicton (c). Although calculated first eigenvalue λ_1 is only 0.43, there are convincing subhorizontal to low oblique signals visible. Example of moderately to well-developed unistrial to masepic plasmic fabrics (preferred clay mineral orientations shown by white arrows) (cross-polarized light; width of view 4 mm) (d). Such unidirectional plasmic fabrics are normally attributed to simple shear deformation.

observed (Fig. 6b), both of which can be taken as evidence of simple shear deformation (see Hiemstra and Rijsdijk, 2003). μCT analysis was also used to corroborate the suggested micro-fabric signal. Two samples, each consisting of several thousands of grains, show that there are subhorizontal modes in the micro-fabric (Fig. 6c), although the calculated eigenvalues are only moderately strong. It is reasonable to assume that the signals reflect some form of flow or strain and are related either to depositional or to deformational processes.

The predominantly silty matrix is heterogeneous, where there are zones enriched in clay around large pebbles (possibly related to granite weathering) and other parts that are distinctly sandier. In some places, a network of silty to sandy 'tracks' delineate diamictic aggregates, which is probably the reason for the fragmented nature of the diamicton. The tracks look flushed or have a fluidized appearance and they seem to be associated with the irregularly shaped pores and fractures described above. There is also evidence of clay illuviation in pores, which together with the tracks strongly suggest water circulation in the diamicton, most probably post-depositionally. In cross-polarized light, the diamicton shows patterns of unidirectional birefringence (plasmic fabrics; see Hiemstra, 2013), which reflects narrow zones of preferentially aligned clay particles (Fig. 6d) and are generally taken as evidence of strain within the sediment. This is probably in response to syn-depositional simple shear deformation. The orientation of the plasmic fabrics often conforms to the preferred micro-fabrics observed.

Overall, the micro-scale characteristics of the Scilly Rock diamicton strongly suggest that post-depositional processes have played a major role in the formation of the characteristics of this sediment (see also Hiemstra and Carr, 2015). Firstly, there is evidence of *in situ* weathering of granite clasts (including the alteration of biotite minerals to clays). Secondly, there is ample evidence of water movement probably occurring post-depositionally, not syn-depositionally, within

the diamicton based on the irregular nature of pore spaces, the localized effects of winnowing and fluidization, and traces of clay illuviation. There is also strong microscopic evidence of 'primary' strain, which is localized but consistent in terms of overall character. The geometric planar fracture patterns and the identified types of fabrics are compatible in terms of general orientations with a simple, syn-depositional shearing regime. The micro-fabric modes, the unidirectional plasmic fabrics and their close association with turbates would be consistent with a subglacial shearing environment (see van der Meer, 1993; van der Meer and Menzies, 2011; and references therein). This suggests that the diamicton analysed represents a basal till or a subglacial traction till (cf. Evans *et al.*, 2006b) that has been post-depositionally modified.

Age constraints

The three TCN samples overlying the diamicton from Scilly Rock yielded apparent exposure ages of 26.7 ± 1.6, 44.8 ± 2.5 and 25.0 ± 1.5 ka (Table 2). Given the age correspondence (within their analytical uncertainties) of two of the samples, the oldest age (T4SCI02) appears to be an outlier and is attributed to nuclide inheritance. Samples T4SCI01 and T4SCI03 have exposure ages that agree within their analytical uncertainties (Table 2). While their geomorphological context does not allow their previous orientation to be inferred, their ages imply mobilization around the time of the LGM. Also, the boulders from which these samples were taken directly overlie erratic-bearing diamicton (see 'Diamicton' above), which shows that there is probably a direct relationship between the boulder and the glacial deposits. If this is the case, and considering the potential for inheritance (see 'Shipman Head, Bryher' above), then the remaining two Scilly Rock exposure ages constrain the timing of the LGM on the Isles of Scilly to an arithmetic mean age of 25.9 ± 1.6 ka with a range of 28.3–23.5 ka.

Tresco

Previous OSL studies of glacial sediments from the Isles of Scilly (Scourse and Rhodes, 2006) have reported issues with feldspar contamination in the density-separated quartz fractions. Single-grain OSL measurements of the quartz fraction separated in this study show that ~5% of the grains gave D_e values, but ~40% of these grains failed the OSL-IR depletion ratio test (Duller, 2003), which addressed issues of feldspar contamination. Typical decay curves and a dose–response curve measured for a single grain of quartz from sample T4BATT03 are shown in Fig. 7. The D_e values for single grains of quartz that passed the OSL-IR depletion ratio test (and the other criteria described above) from all five samples gave overdispersion values ranging from 37 to 43% (Fig. 8). The single-grain D_e values determined for the samples in this study are included in Tables S3–S7. The central age model (CAM) was used to determine OSL ages for these samples (Table 1) as the symmetrical distribution of D_e values did not suggest that the grains were heterogeneously bleached before burial (Fig. 8). OSL ages of 29.1 ± 1.9, 26.8 ± 2.0, 22.5 ± 1.8 and 23.7 ± 2.0 ka were determined for samples T4BATT01, T4BATT03, T4BATT04 and T4BATT05, respectively (Table 1) and constrain the deposition of the Tregarthen Gravel at Battery. The OSL age of 19.6 ± 1.5 ka for the overlying sample (T4BATT06) then determined the timing of deposition of the Hell Bay Gravel. The three TCN samples from Gunhill on Tresco associated with the OSL samples yielded apparent exposure ages of 52.9 ± 3.0 and 30.4 ± 1.8 ka (both granite boulders) and 25.3 ± 1.5 ka (quartzite erratic).

Discussion

The TCN concentration measured from the underside of the Shipman Head boulder and the existing TCN exposure ages from outside the inferred ice limit (McCarroll *et al.*, 2010) indicate that the granite tors of the Isles of Scilly have a long exposure history, increasing the likelihood of nuclide inheritance in the TCN samples. This fact is highlighted by the ages presented for samples T4SCI02 and T4TRE01, which pre-date the LGM. The long exposure history highlights the potential for significant muonic contributions to ^{10}Be inventories measured in large overturned boulders, demonstrated by the exposure ages obtained from the upper surface of the Shipman Head boulder (see 'Shipman Head,

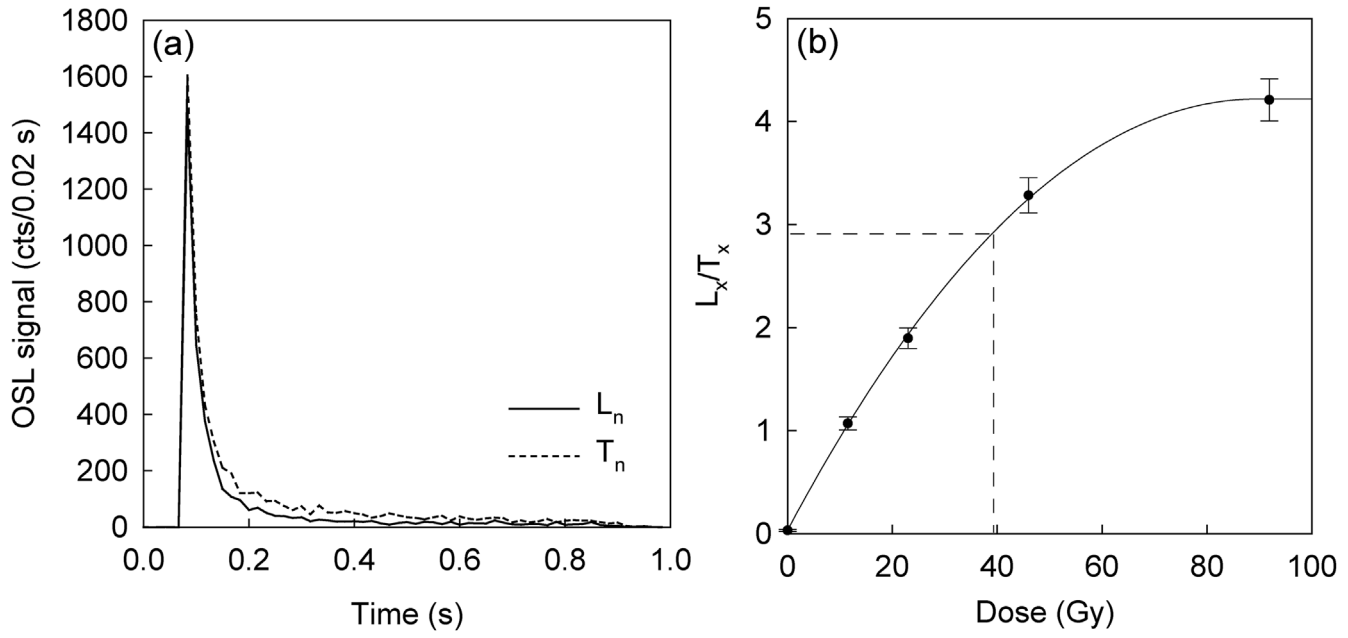

Figure 7. Examples of typical decay curves (a) and a dose–response curve (b) for a single grain of quartz from sample T4BATT03. The test-dose used in this study was 9.5 Gy.

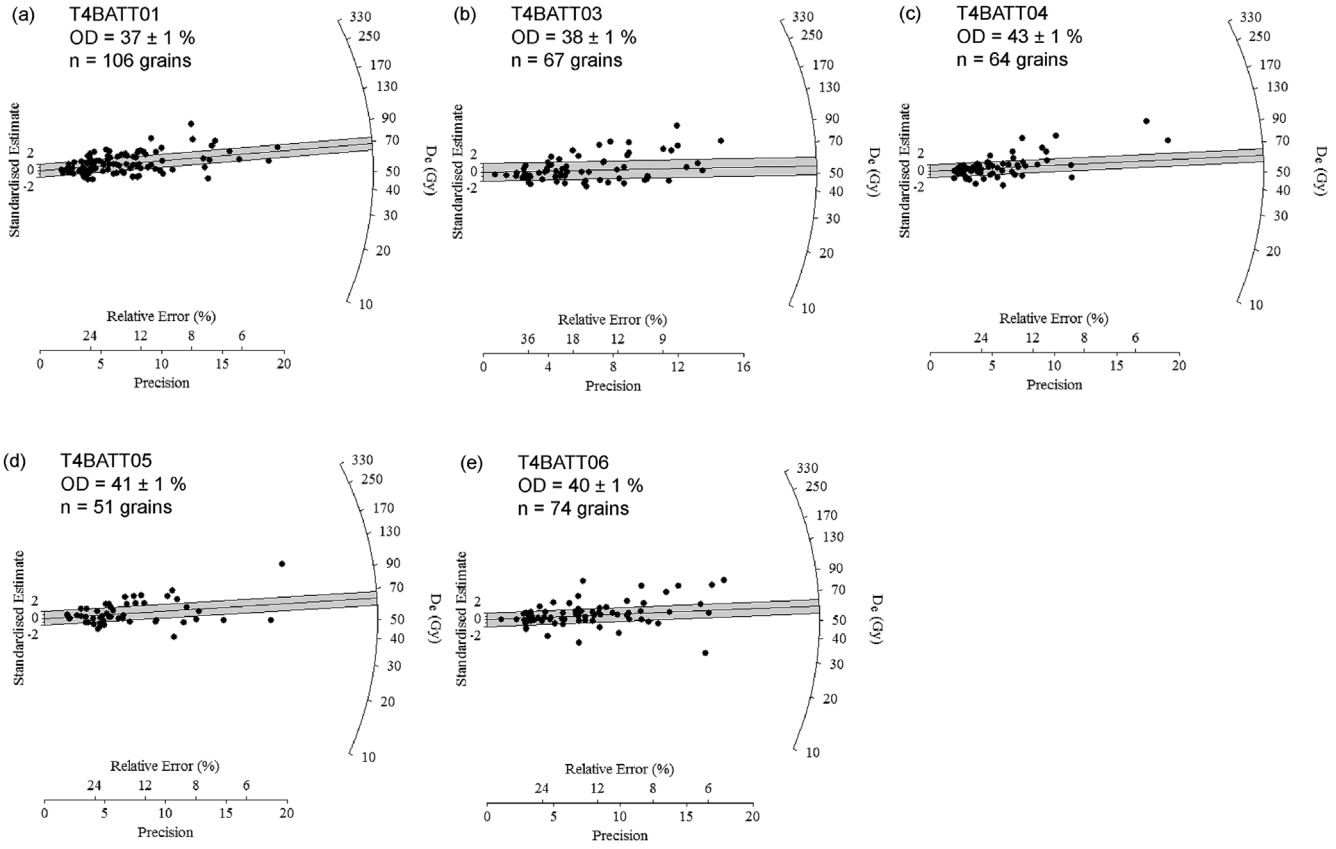

Figure 8. Radial plots for the single-grain D_e values determined from the samples in this study using OSL dating of quartz. The single-grain D_e values determined for the samples in this study are included in Tables S3–S7.

Bryher' in the Results). These ages include roughly 20 000 ^{10}Be atoms g^{-1}, equivalent to ~5 ka of full exposure, acquired before overturning. An age of 19–17 ka for deposition of the boulder at Shipman Head suggests that glaciation is an unlikely agent of boulder mobilization at this time as the ISIS is known to have retreated ~500 km north of the Isles of Scilly to the Isle of Man by ~17 ka (Chiverrell *et al.*, 2013). Consequently, an alternative mechanism(s) must be responsible for overturning this boulder, such as periglacial activity or the highly energetic storm waves known to influence the Isles of Scilly (e.g. Fig. 4a), and the usage of the term 'boulder moraine' to describe the Shipman Head feature should be discontinued.

Although the potential for nuclide inheritance suggests that caution needs to be applied when interpreting exposure ages, there is supporting geomorphological and sedimentary evidence that can be used to draw some inferences on when the ISIS impinged on to the northern Isles of Scilly. The inference that ice was responsible for mobilization of the boulder sampled for T4TRE02 (see 'sample sites', 'Scilly Rock') is not refuted by the apparent exposure age obtained from its top surface of 30.4 ± 1.8 ka. Although this age pre-dates the LGM, the boulder appears to be overturned due to the absence of weathering features on its top surface and it is likely to contain a significant muonic contribution (see 'Shipman Head, Bryher' in the Results), thus overestimating the time elapsed since boulder mobilization by an indeterminable amount. The age therefore represents a maximum limit on the timing of glaciation of the Isles of Scilly.

The youngest exposure age from Tresco (T4TRE03) was obtained from an erratic quartzite clast sampled from the surface within the maximum extent of the Hell Bay Gravel (Scourse, 1991). Considering that the clast was exposed at the present-day surface, it is likely that it was covered by overlying material to some degree in the past. This would act to attenuate the incoming cosmic radiation, reducing the production rate of ^{10}Be within the sample and resulting in an apparent exposure age that underestimates the true age of deposition. Although the depth and duration of cover cannot be quantified, the extremely low relief of the sample site precludes significant erosion of material implying that any pre-existing cover was probably thin. As a result, the exposure age is not corrected for any post-depositional shielding and the resulting age is interpreted as a minimum. The Isles of Scilly are composed entirely of Variscan granite and so the quartzite erratic was most likely deposited by the ISIS when it impinged upon the northern Isles of Scilly. The exposure age of 25.3 ± 1.5 ka for sample T4TRE03 is interpreted as a minimum limit on the timing of glaciation of the Isles of Scilly.

The boulders from which samples T4SCI01 and T4SCI03 were collected both directly overlie glacigenic sediments (see 'Sample sites'). While the potential for nuclide inheritance cannot be discounted, the good agreement of these ages and their sedimentological association suggest that their exposure ages represent boulder mobilization by ice. Additionally, these ages are bracketed by the maximum and minimum limiting age control provided by the ages from Tresco, which adds further chronological constraints to the last glaciation of the Isles of Scilly. As a result, the TCN data suggest that the ISIS extended to the Isles of Scilly during a time interval after 30.4 ± 1.8 ka and before 25.3 ± 1.5 ka. This agrees with the exposure ages from Scilly Rock (T4SCI01 and T4SCI03), which suggest ice impinged on the Isles of Scilly at 28.3–23.5 ka, with an arithmetic mean age of 25.9 ± 1.6 ka.

The new OSL ages for the deposition of the Tregarthen Gravel associated with the Scilly Till (Scourse, 1991) at Battery (Fig. 3) also suggest that ice was impinging on the

Isles of Scilly during MIS 2 (Table 1). Although the reliability of the preliminary ages reported by Scourse and Rhodes (2006) for the Tregarthen Gravel at Battery is difficult to assess due to the lack of information published for the analyses, the ages of 25.1 ± 2.2 and 22.7 ± 0.9 ka are consistent with the new OSL ages in this study.

The OSL ages of samples taken from the Tregarthen Gravel in this study are not in simple stratigraphic order (Fig. 3). This is unlikely to have been caused by inaccurate environmental dose-rates as these have been independently assessed using multiple methods in this study (see 'OSL dating'). Inaccurate estimation of the water content throughout burial is also unlikely as samples were taken from within 1 m of each other in the same stratigraphic section with identical overlying and underlying sedimentary units of breccia (Fig. 3c). The OSL ages are consistent with each other within $\pm 2\sigma$, and this probably reflects the reproducibility of OSL dating of replicate samples from a single depositional event. An approach to determine an OSL age for the ice advance to the Isles of Scilly indicated by the Tregarthen Gravel is therefore to calculate the weighted mean and standard error of the four OSL ages (25.5 ± 1.5 ka), where the standard error was calculated using equations 21 and 22 of Aitken and Alldred (1972).

The weighted mean of the OSL ages for the Tregarthen Gravel at Battery (25.5 ± 1.5 ka) agrees with the TCN exposure ages from boulders on Scilly Rock (25.9 ± 1.6 ka), and provides strong evidence that sediments were deposited by ice during MIS 2 (Fig. 2). The OSL and TCN ages for ice advance to the northern Isles of Scilly suggest that it occurred around the time of maximum position at 25.4–24.0 cal ka BP reported for the south coast of Ireland from the youngest radiocarbon ages for reworked shell fragments within subglacial Irish Sea diamicton (Ó Cofaigh and Evans, 2007). OSL ages for proglacial outwash in southern Ireland at Whiting Bay (24.4 ± 1.8 ka; 24.2 ± 2.3 ka) and Ballycroneen (23.8 ± 2.1 ka; 21.6 ± 2.1 ka) (Ó Cofaigh *et al.*, 2012) then suggest rapid retreat of the ISIS from its maximum position in the Celtic Sea to south-eastern Ireland at 23.7–22.9 ka (Fig. 9; Chiverrell *et al.*, 2013), and thus retreated more rapidly than the subsequent retreat of the ISIS northwards to the Isle of Man (Chiverrell *et al.*, 2013). While the ISIS was rapidly retreating from the Isles of Scilly to the coasts of south-east Ireland and south-west Wales, ice masses in Ireland (e.g. Ballantyne and Stone, 2015) and Wales (e.g. Hughes *et al.*, 2016) are reported to have rapidly thinned.

The terrestrial signature for an ice advance to the northern Isles of Scilly constrained by the OSL (25.5 ± 1.5 ka) and TCN (25.9 ± 1.6 ka) ages suggests that the maximum extent of the ISIS in the Celtic Sea coincided with global LGM (Fig. 9; Clark *et al.*, 2009). Ice impingement on to the Isles of Scilly ended around the time of Heinrich Event 2 (H2) ~24 ka as the ISIS ice front was in south-east Ireland 23.7–22.9 ka (Fig. 9; Chiverrell *et al.*, 2013). This is shown in the IRD record from the marine core OMEX-2K at Goban Spur by an increase in IRD flux from the ISIS at ~24 ka (Fig. 9; Scourse *et al.*, 2009a; Haapaniemi *et al.*, 2010). The

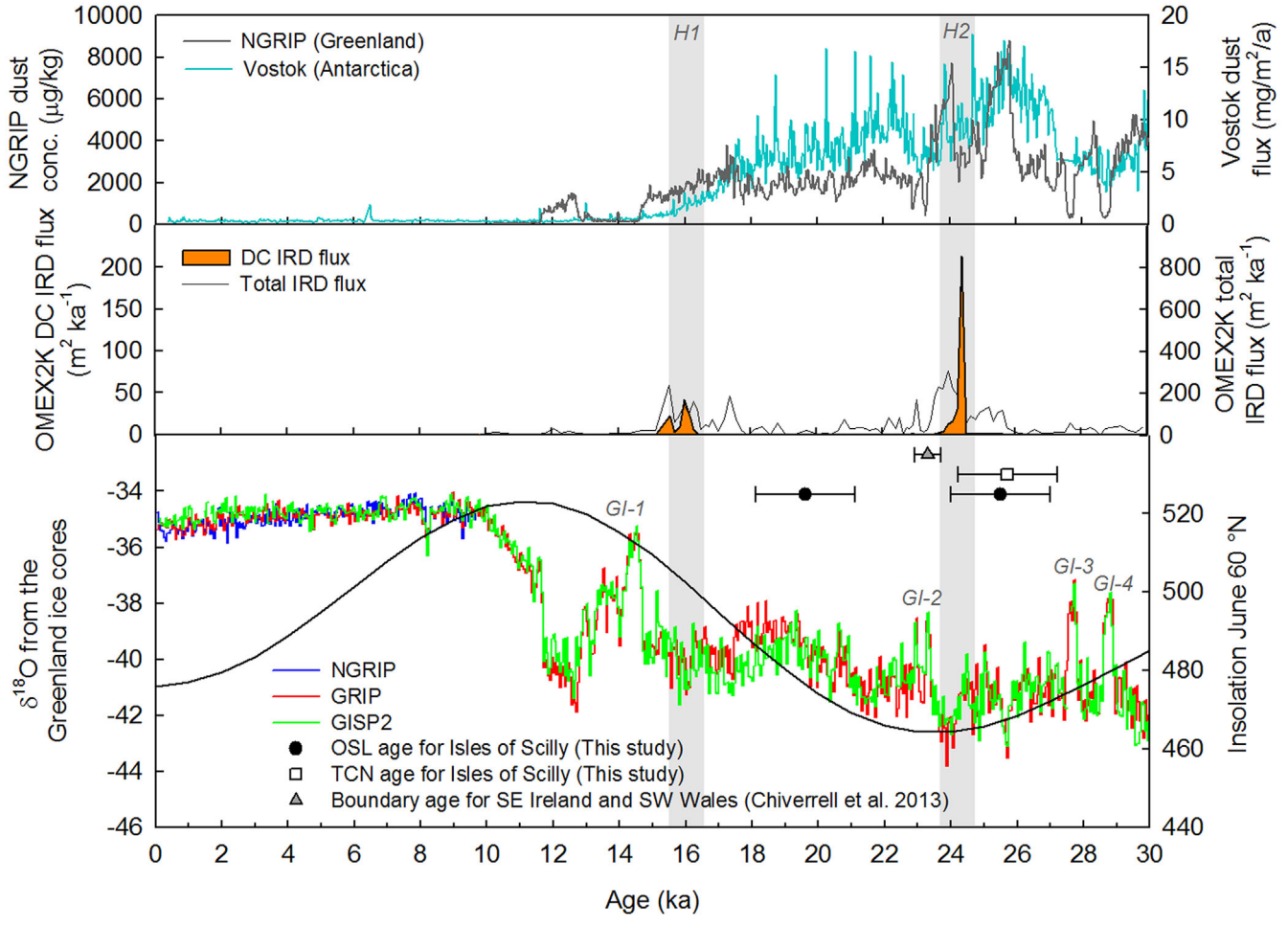

Figure 9. Plotted alongside the OSL and TCN ages determined in this study are the $\delta^{18}O$ records and Greenland interstadials as identified from the Greenland ice cores presented in Rasmussen *et al.* (2014) plotted using the Greenland Ice Core Chronology GICC05 (b2k), summer isolation (Berger and Loutre, 1991), records of dolomitic carbon (DC) and total IRD flux from the OMEX2K marine core with radiocarbon age model tuned to GISP2 (Haapaniemi *et al.*, 2010), and the dust records obtained from the NGRIP (Ruth *et al.*, 2007) and Vostok (Lambert *et al.*, 2012) ice cores. The grey shading marks Heinrich Events H1 and H2 (after Bond *et al.*, 1992).

marine record at Goban Spur documents a decrease in salinity immediately following H2, which may be linked to ISIS deglaciation (Haapaniemi *et al.*, 2010). Rapid recession of the ISIS followed the ice advance during the marked warming of Greenland Interstadial 2 (GI-2; ~23 ka) (Fig. 9). It is likely that a combination of factors contributed towards the rapid retreat of the ISIS from its maximum extent in the Celtic Sea to south-eastern Ireland; these include glacio-eustatic forcing linked to H2, ocean and atmospheric warming (Scourse *et al.*, 2009a; Haapaniemi *et al.*, 2010), a megatidal regime (Scourse *et al.*, 2009b), destabilization and potential overextension of the ISIS after the short-lived advance that would have sustained a wider and more active calving margin (Hubbard *et al.*, 2009).

OSL dating of the Hell Bay Gravel at Battery suggests that this site was ice-free at 19.6 ± 1.5 ka. This is consistent with the Bayesian model for the retreat of the ISIS that suggests the ice front had retreated ~400 km northwards to Anglesey in Wales by ~20 ka (Chiverrell *et al.*, 2013). Comparing the OSL age for the Hell Bay Gravel with the TL (18.6 ± 3.7 ka; Wintle, 1981) and OSL (20 ± 7 ka; Smith *et al.*, 1990) ages for the Old Man Sandloess supports the suggestion by Scourse *et al.* (2006) that both units represent post-glacial deposition on the Isles of Scilly at a similar time. However, the original ages from the Old Man Sandloess were determined using experimental methods and so these samples need to be re-visited using modern OSL dating protocols (e.g. the SAR protocol; Murray and Wintle, 2000) to increase confidence in this comparison.

After deposition of the Scilly Till and Tregarthen Gravel in the northern Isles of Scilly (Fig. 2), the OSL age of the Hell Bay Gravel (19.6 ± 1.5 ka) suggests there was a delay of ~5 ka between primary glacigenic deposition and aeolian reworking of this material. This occurred around a similar time to the overturning of the boulder at Shipman Head (see Results, 'Shipman Head, Bryher'). At present, there are no stratigraphic or geochronological data to inform the character of landscape evolution on the Isles of Scilly during the ~5-ka lacuna between primary glacigenic deposition and aeolian reworking. At ~20 ka, the ISIS ice front was known to be oscillating on and around the Llŷn Peninsula (Thomas and Chiverrell, 2007; Chiverrell *et al.*, 2013), which was at a similar time to the deposition of the Old Man Sandloess.

There is evidence on the Isles of Scilly for a phase of intense solifluction and ploughing block emplacement following the primary deposition of the Old Man Sandloess ~20 ka (Scourse, 1991). This is represented by the Bread and Cheese Breccia north of the ice limit and the upper Porthloo Breccia to the south of the ice limit (Fig. 2). The OSL age for the Old Man Sandloess provides a maximum age for this final phase of solifluction. It is also worth noting that the revised age of ~19–17 ka for the Shipman Head boulder coincides with the period immediately following the deposition of the Old Man Sandloess. This raises the possibility that the boulder accumulation on Shipman Head is a remanié collection of soliflucted or ploughing blocks derived from the adjacent tor. Any matrix associated with the boulder accumulation has been subsequently removed by wave action in this exposed context (Fig. 4b), similar to the partial removal of the diamicton matrix associated with the boulders on Scilly Rock. The phase of solifluction that followed aeolian reworking of the glacigenic sediments may have also occurred during the period ~20 ka when the ISIS ice front was oscillating on and around the Llŷn Peninsula (Thomas and Chiverrell, 2007; Chiverrell *et al.*, 2013), but could also be much younger, possibly even Lateglacial in age (Scourse, 1991).

Conclusions

The new ages reported in this study in combination with previous work provide strong evidence that ice advanced to the Isles of Scilly during MIS 2. The OSL age of 25.5 ± 1.5 ka for the deposition of ice-marginal outwash sediments at Battery, the limiting TCN exposure ages of 30.4 ± 1.8 and 25.3 ± 1.5 ka from northern Tresco, and the mean TCN exposure age of 25.9 ± 1.6 ka from boulders directly overlying till on Scilly Rock suggest that ice was impinging on the northern Isles of Scilly earlier than was previously estimated by Chiverrell *et al.* (2013). This implies that ice impingement on to the Isles of Scilly ended around the time of increased IRD flux in the marine record at ~24 ka associated with H2. This supports the suggestions of previous studies that ice advance and retreat on to the Isles of Scilly was related to H2 and was followed by recession of the ISIS during the warming of the GI-2 at ~23 ka. After the ISIS had receded from the Isles of Scilly, there was a delay of ~5 ka between the primary deposition and aeolian reworking of glacigenic sediment according to the OSL age of 19.6 ± 1.5 ka for the Hell Bay Gravel. At present, there is a lack of evidence for the environmental history of the Isles of Scilly after the advance of ice and before the phase of aeolian deposition, during a time when the ISIS ice front is known to have been oscillating on and around the Llŷn Peninsula, Wales. This phase of aeolian activity was then followed by a phase of active solifluction.

Acknowledgements. This paper was supported by a Natural Environment Research Council consortium grant (BRITICE-CHRONO NE/J008672/1). H. Wynne is thanked for etching the quartz grains for OSL dating. A. Palmer and S. Carr are also acknowledged for preparing the thin sections and running the tomograph analyses, respectively. Thanks to the Tresco Estate for allowing us access to the Battery and Gunhill sites and facilitating sampling there, to Dave Mawer and Julie Love of the IOS Wildlife Trust for facilitating access to Shipman Head and Scilly Rock, and for supplying the photograph (Fig. 4b). We would like to thank Jeremy Phillips of the St Mary's Boatmen's Association for logistical support.

Supporting Information

Table S1. Details of the ages determined from previous studies on the Isles of Scilly.

Table S2. Chemistry and AMS data for samples from the Isles of Scilly.

Table S3. D_e values from OSL dating of sample T4BATT01 from the Isles of Scilly.

Table S4. D_e values from OSL dating of sample T4BATT03 from the Isles of Scilly.

Table S5. D_e values from OSL dating of sample T4BATT04 from the Isles of Scilly.

Table S6. D_e values from OSL dating of sample T4BATT05 from the Isles of Scilly.

Table S7. D_e values from OSL dating of sample T4BATT06 from the Isles of Scilly.

Abbreviations. AMS, accelerator mass spectrometry; BIIS, British–Irish Ice Sheet; GI-2, Greenland Interstadial 2; GRPR, Glen Roy production rate; H2, Heinrich Event 2; ICP-AES, inductively coupled plasma atomic emission spectroscopy; ICP-MS, inductively coupled plasma mass spectrometry; IRD, ice-rafted debris; ISIS, Irish Sea Ice Stream; LLPR, Loch Lomond production rate; MIS, Marine Isotope Stage; OSL, optically stimulated luminescence; TCN, terrestrial cosmogenic nuclide; TL, thermoluminescence; μCT, micro-X-ray tomography.

References

Aitken MJ, Alldred JC. 1972. The assessment of error limits in thermoluminescent dating. *Archaeometry* **14**: 257–267 [DOI: 10.1111/j.1475-4754.1972.tb00068.x].

Balco G, Briner J, Finkel RC *et al*. 2009. Regional beryllium-10 production rate calibration for late-glacial northeastern North America. *Quaternary Geochronology* **4**: 93–107 [DOI: 10.1016/j.quageo.2008.09.001].

Balco G, Stone JO, Lifton NA *et al*. 2008. A complete and easily accessible means of calculating surface exposure ages or erosion rates from ^{10}Be and ^{26}Al measurements. *Quaternary Geochronology* **3**: 174–195 [DOI: 10.1016/j.quageo.2007.12.001].

Ballantyne CK. 2001. Measurement and theory of boulder ploughing movement. *Permafrost and Periglacial Movement* **12**: 267–288.

Ballantyne CK, Stone JO. 2015. Trimlines, blockfields and the vertical extent of the last ice sheet in southern Ireland. *Boreas* **44**: 277–287 [DOI: 10.1111/bor.12109].

Barrow G. 1906. *The Geology of the Isles of Scilly. Memoirs of the Geological Survey of Great Britain*. HMSO: London.

Berger A, Loutre MF. 1991. Insolation values for the climate of the last 10000000 years. *Quaternary Science Reviews* **10**: 297–317.

Bond G, Heinrich H, Broecker W *et al*. 1992. Evidence for massive discharges of icebergs into the North Atlantic Ocean during the last glacial period. *Nature* **360**: 245–249 [DOI: 10.1038/360245a0].

Bøtter-Jensen L, Andersen CE, Duller GAT *et al*. 2003. Developments in radiation, stimulation and observation facilities in luminescence measurements. *Radiation Measurements* **37**: 535–541 [DOI: 10.1016/S1350-4487(03)00020-9].

Bowen DQ. 1973. The Pleistocene succession of the Irish Sea. *Proceedings of the Geologists' Association* **84**: 249–IN2 [DOI: 10.1016/S0016-7878(73)80034-3].

Bowen DQ. 1999. Only four major 100-ka glaciations during the Brunhes Chron? *International Journal of Earth Sciences* **88**: 276–284 [DOI: 10.1007/s005310050264].

Braucher R, Brown ET, Bourlès DL *et al*. 2003. *In situ* produced ^{10}Be measurements at great depths: implications for production rates by fast muons. *Earth and Planetary Science Letters* **211**: 251–258 [DOI: 10.1016/S0012-821X(03)00205-X].

Brück PM, Reeves TJ. 1976. Stratigraphy, sedimentology and structure of the Bray Group in County Wicklow and south County Dublin. *Proceedings of the Royal Irish Academy Section B: Biological, Geological, and Chemical Science* **76**: 53–77.

Chiverrell RC, Thrasher IM, Thomas GSP *et al*. 2013. Bayesian modelling the retreat of the Irish Sea Ice Stream. *Journal of Quaternary Science* **28**: 200–209 [DOI: 10.1002/jqs.2616].

Clark PU, Dyke AS, Shakun JD *et al*. 2009. The Last Glacial Maximum. *Science* **325**: 710–714 [DOI: 10.1126/science.1172873] [Pubmed:19661421].

Child D, Elliot G, Mifsud C, Smith AM, Fink D. 2000. Sample processing for earth science studies at ANTARES. *Nuclear Instruments and Methods in Physics Research Section B: Beam Interactions with Materials and Atoms* **172**: 856–860.

Coque-Delhuille B, Veyret Y. 1984. La limite de l'englacement Quaternaire dans le Sud-Ouest Anglais (Grande Bretagne). *Revue de Géomorphologique Dynamique* **33**: 1–24.

Coque-Delhuille B, Veyret Y. 1989. Limite d'englacement et évolution périglaciaire des Iles Scilly: l'intérêt des arènes *in situ* et remaniées. *Zeitschrift für Geomorphologie* **72**: 79–96.

Duller GAT. 2003. Distinguishing quartz and feldspar in single grain luminescence measurements. *Radiation Measurements* **37**: 161–165 [DOI: 10.1016/S1350-4487(02)00170-1].

Durcan JA, King GE, Duller GAT. 2015. DRAC: Dose Rate and Age Calculator for trapped charge dating. *Quaternary Geochronology* **28**: 54–61 [DOI: 10.1016/j.quageo.2015.03.012].

Granger DE, Smith AL. 2000. Dating buried sediments using radioactive decay and muogenic production of 26Al and ^{10}Be. *Nuclear Instruments and Methods in Physics Research Section B: Beam Interactions with Materials and Atoms* **172**: 822–826 [DOI: 10.1016/S0168-583X(00)00087-2].

Evans DJA, Ó Cofaigh CÓ. 2003. Depositional evidence for marginal oscillations of the Irish Sea ice stream in southeast Ireland during the last glaciation. *Boreas* **32**: 76–101 [DOI: 10.1111/j.1502-3885.2003.tb01443.x].

Evans DJA, Phillips ER, Hiemstra JF *et al*. 2006b. Subglacial till: formation, sedimentary characteristics and classification. *Earth-Science Reviews* **78**: 115–176 [DOI: 10.1016/j.earscirev.2006.04.001].

Evans DJA, Scourse JD, Hiemstra JF *et al*. 2006a. Bread and Cheese Cove. In *Isles of Scilly. Field Guide*, Scourse JD (ed.). Quaternary Research Association: London; 111–122.

Fabel D, Ballantyne CK, Xu S. 2012. Trimlines, blockfields, mountain-top erratics and the vertical dimensions of the last British–Irish Ice Sheet in NW Scotland. *Quaternary Science Reviews* **55**: 91–102 [DOI: 10.1016/j.quascirev.2012.09.002].

Fenton CR, Hermanns RL, Blikra LH *et al*. 2011. Regional ^{10}Be production rate calibration for the past 12ka deduced from the radiocarbon-dated Grøtlandsura and Russenes rock avalanches at 69° N, Norway. *Quaternary Geochronology* **6**: 437–452 [DOI: 10.1016/j.quageo.2011.04.005].

Goehring BM, Lohne ØS, Mangerud J *et al*. 2012b. Erratum: Late glacial and Holocene ^{10}Be production rates for western Norway. *Journal of Quaternary Science* **27**: 544–544 [DOI: 10.1002/jqs.2548].

Goehring BM, Lohne ØS, Mangerud J *et al*. 2012a. Late glacial and Holocene ^{10}Be production rates for western Norway. *Journal of Quaternary Science* **27**: 89–96 [DOI: 10.1002/jqs.1517].

Guerin G, Mercier N, Adamiec G. 2011. Dose-rate conversion factors: update. *Ancient TL* **29**: 5–8.

Guérin G, Mercier N, Nathan R *et al*. 2012. On the use of the infinite matrix assumption and associated concepts: a critical review. *Radiation Measurements* **47**: 778–785 [DOI: 10.1016/j.radmeas.2012.04.004].

Haapaniemi AI, Scourse JD, Peck VL *et al*. 2010. Source, timing, frequency and flux of ice-rafted detritus to the northeast Atlantic margin, 30–12 ka: testing the Heinrich precursor hypothesis. *Boreas* **39**: 576–591.

Hiemstra JF. 2013. Micromorphology of glacial sediments. In *The Encyclopedia of Quaternary Science*, Vol. **2**, Elias SA (ed.). Elsevier: Amsterdam; 52–61.

Hiemstra JF, Carr SJ. 2015. Microscopic analyses of a diamicton from Scilly Rock (SV85916) –contextual information for the BRITICE-CHRONO project. Centre for Micromorphology Report no. 11.

Hiemstra JF, Evans DJA, Scourse JD *et al*. 2006. New evidence for a grounded Irish Sea glaciation of the Isles of Scilly, UK. *Quaternary Science Reviews* **25**: 299–309 [DOI: 10.1016/j.quascirev.2005.01.013].

Hiemstra JF, Rijsdijk KF. 2003. Observing artificially induced strain: implications for subglacial deformation. *Journal of Quaternary Science* **18**: 373–383 [DOI: 10.1002/jqs.769].

Hubbard A, Bradwell T, Golledge N *et al*. 2009. Dynamic cycles, ice streams and their impact on the extent, chronology and deglaciation of the British–Irish ice sheet. *Quaternary Science Reviews* **28**: 758–776 [DOI: 10.1016/j.quascirev.2008.12.026].

Hughes PD, Glasser NF, Fink D. 2016. Rapid thinning of the Welsh Ice Cap at 20–19 ka based on ^{10}Be ages. *Quaternary Research* **85**: 107–117 [DOI: 10.1016/j.yqres.2015.11.003].

Kaplan MR, Strelin JA, Schaefer JM *et al*. 2011. In-situ cosmogenic ^{10}Be production rate at Lago Argentino, Patagonia: implications for late-glacial climate chronology. *Earth and Planetary Science Letters* **309**: 21–32 [DOI: 10.1016/j.epsl.2011.06.018].

Lal D. 1991. Cosmic ray labeling of erosion surfaces: *in situ* nuclide production rates and erosion models. *Earth and Planetary Science Letters* **104**: 424–439 [DOI: 10.1016/0012-821X(91)90220-C].

Lambert F, Bigler M, Steffensen JP *et al*. 2012. Centennial mineral dust variability in high-resolution ice core data from Dome C, Antarctica. *Climate of the Past* **8**: 609–623 [DOI: 10.5194/cp-8-609-2012].

MacLeod A, Matthews IP, Lowe JJ *et al*. 2015. A second tephra isochron for the Younger Dryas period in northern Europe: the Abernethy Tephra. *Quaternary Geochronology* **28**: 1–11 [DOI: 10.1016/j.quageo.2015.03.010].

MacLeod A, Palmer A, Lowe J *et al*. 2011. Timing of glacier response to Younger Dryas climatic cooling in Scotland. *Global and Planetary Change* **79**: 264–274 [DOI: 10.1016/j.gloplacha.2010.07.006].

McCabe AM. 2008. *Glacial Geology and Geomorphology: the Landscapes of Ireland*. Dunedin Academic Press: Edinburgh.

McCarroll D, Stone JO, Ballantyne CK *et al*. 2010. Exposure-age constraints on the extent, timing and rate of retreat of the last Irish Sea ice stream. *Quaternary Science Reviews* **29**: 1844–1852 [DOI: 10.1016/j.quascirev.2010.04.002].

Mitchell GF, Orme AR. 1967. The Pleistocene deposits of the Isles of Scilly. *Quarterly Journal of the Geological Society* **123**: 59–92 [DOI: 10.1144/gsjgs.123.1.0059].

Murray AS, Wintle AG. 2000. Luminescence dating of quartz using an improved single-aliquot regenerative-dose protocol. *Radiation Measurements* **32**: 57–73 [DOI: 10.1016/S1350-4487(99)00253-X].

Ó Cofaigh C, Evans DJA. 2001a. Deforming bed conditions associated with a major ice stream of the last British ice sheet. *Geology* **29**: 795–798 [DOI: 10.1130/0091-7613(2001)029<0795:DBCAWA>2.0.CO;2].

Ó Cofaigh C, Evans DJA. 2001b. Sedimentary evidence for deforming bed conditions associated with a grounded Irish Sea glacier, southern Ireland. *Journal of Quaternary Science* **16**: 435–454.

Ó Cofaigh C, Evans DJA. 2007. Radiocarbon constraints on the age of the maximum advance of the British–Irish Ice Sheet in the Celtic Sea. *Quaternary Science Reviews* **26**: 1197–1203 [DOI: 10.1016/j.quascirev.2007.03.008].

Ó Cofaigh C, Telfer MW, Bailey RM *et al.* 2012. Late Pleistocene chronostratigraphy and ice sheet limits, southern Ireland. *Quaternary Science Reviews* **44**: 160–179 [DOI: 10.1016/j.quascirev.2010.01.011].

Palmer AP, Lee JA, Kemp RA *et al.* 2008. *Revised Laboratory Procedures for the Preparation of Thin Sections from Unconsolidated Sediments*. Centre for Micromorphology unpublished report.

Phillips E. 1991. The lithostratigraphy, sedimentology and tectonic setting of the Monian Supergroup, western Anglesey, North Wales. *Journal of the Geological Society* **148**: 1079–1090 [DOI: 10.1144/gsjgs.148.6.1079].

Phillips FM, Argento DC, Balco G *et al.* 2016. The CRONUS-Earth project: a synthesis. *Quaternary Geochronology* **31**: 119–154 [DOI: 10.1016/j.quageo.2015.09.006].

Praeg D, McCarron S, Dove D *et al.* 2015. Ice sheet extension to the Celtic Sea shelf edge at the last glacial maximum. *Quaternary Science Reviews* **111**: 107–112 [DOI: 10.1016/j.quascirev.2014.12.010].

Prescott JR, Hutton JT. 1994. Cosmic ray contributions to dose rates for luminescence and ESR dating: large depths and long-term time variations. *Radiation Measurements* **23**: 497–500 [DOI: 10.1016/1350-4487(94)90086-8].

Putnam AE, Schaefer JM, Barrell DJA *et al.* 2010. *In situ* cosmogenic ^{10}Be production-rate calibration from the Southern Alps, New Zealand. *Quaternary Geochronology* **5**: 392–409 [DOI: 10.1016/j.quageo.2009.12.001].

Rasmussen SO, Bigler M, Blockley SP, Blunier T, Buchardt SL, Clausen HB, Cvijanovic I, Dahl-Jensen D, Johnsen SJ, Fischer H, Gkinis V, Guillevic M, Hoek WZ, Lowe JJ, Pedro JB, Popp T, Seierstad IK, Steffensen JP, Svensson AM, Vallelonga P, Vinther BM, Walker MJC, Wheatley JJ, Winstrup M. 2014. A stratigraphic framework for abrupt climatic changes during the Last Glacial period based on three synchronized Greenland ice-core records: refining and extending the INTIMATE event stratigraphy. *Quaternary Science Reviews* **106**: 14–28.

Reimer PJ, Bard E, Bayliss A *et al.* 2013. IntCal13 and Marine13 radiocarbon age calibration curves 0–50,000 years cal BP. *Radiocarbon* **55**: 1869–1887 [DOI: 10.2458/azu_js_rc.55.16947].

Ruth U, Bigler M, Röthlisberger R *et al.* 2007. Dust concentration in the NGRIP ice core. *Geophysical Research Letters* **34**: L03706 [DOI: 10.1029/2006GL027876].

Scourse JD. 1991. Late Pleistocene Stratigraphy and Palaeobotany of the Isles of Scilly. *Philosophical Transactions of the Royal Society B: Biological Sciences* **334**: 405–448 [DOI: 10.1098/rstb.1991.0125].

Scourse JD, Austin WEN, Bateman RM *et al.* 1990. Sedimentology and micropalaeontology of glacimarine sediments from the central and southwestern Celtic Sea. *Special Publication of the Geological Society of London* **53**: 329–347.

Scourse JD, Evans DJA, Hiemstra J *et al.* 2006. Pleistocene stratigraphy, geomorphology and geochronology. In *The Isles of Scilly: Field Guide*, Scourse JD (ed.). Quaternary Research Association, London.

Scourse JD, Evans DJA, Hiemstra JF *et al.* 2004. Late Devensian glaciation of the Isles of Scilly: QRA Research Fund Report. *Quaternary Newsletter* **102**: 49–54.

Scourse JD, Furze MFA. 2001. A critical review of the glaciomarine model for Irish Sea deglaciation: evidence from southern Britain, the Celtic shelf and adjacent continental slope. *Journal of Quaternary Science* **16**: 419–434.

Scourse JD, Haapaniemi AI, Colmenero-Hidalgo E *et al.* 2009a. Growth, dynamics and deglaciation of the last British–Irish Ice Sheet: the deep-sea ice-rafted detritus record. *Quaternary Science Reviews* **28**: 3066–3084 [DOI: 10.1016/j.quascirev.2009.08.009].

Scourse JD, Rhodes EJ. 2006. Battery (Castle Down). In *Isles of Scilly. Field Guide*, Scourse JD (ed.). Quaternary Research Association: London; 136–138.

Scourse JD, Uehara K, Wainwright A. 2009b. Celtic Sea linear tidal sand ridges, the Irish Sea Ice Stream and the Fleuve Manche: palaeotidal modelling of a transitional passive margin depositional system. *Marine Geology* **259**: 102–111 [doi:10.1016/j.margeo.2008.12.010].

Small D, Fabel D. 2015. A Lateglacial ^{10}Be production rate from glacial lake shorelines in Scotland. *Journal of Quaternary Science* **30**: 509–513 [DOI: 10.1002/jqs.2804].

Small D, Clark C, Chiverrell RC, Smedley RK, Bateman MB, Duller GAT, Ely JC, Fabel D, Medialdea A, Moreton SG. In Press. Devising quality assurance procedures for assessment of legacy geochronological data relating to deglaciation of the last British-Irish Ice Sheet. *Earth Science Reviews* [DOI: 10.1016/j.earscirev.2016.11.007].

Smith A. 1858. On the chalk flint and greensand fragments found on the Castle Down of Tresco, one of the Islands of Scilly. *Transactions of the Royal Geological Society of Cornwall* **7**: 343–344.

Smith BW, Rhodes EJ, Stokes S *et al.* 1990. Optical dating of sediments: initial quartz results from Oxford. *Archaeometry* **32**: 19–31 [DOI: 10.1111/j.1475-4754.1990.tb01078.x].

Stokes CR, Tarasov L, Blombin R, Cronin T, Fisher TG, Gyllencreutz R, Hättestrand C, Heyman J, Hindmarsh RCA, Hughes ALC, Jakobsson M, Kirchner N, Livingstone SJ, Margold M, Murton JB, Noormets R, Peltier WR, Peteet DM, Piper DJW, Preusser F, Renssen H, Roberts DH, Roche DM, Saint-Ange F, Stroeven AP, Teller JT. 2015. On the reconstruction of palaeo-ice sheets: recent advances and future challenges. *Quaternary Science Reviews* **125**: 15–49.

Stone JO. 2000. Air pressure and cosmogenic isotope production. *Journal of Geophysical Research: Solid Earth* **105**: 23753–23759 [DOI: 10.1029/2000JB900181].

Tarplee MFV, van der Meer JJM, Davis GR. 2011. The 3D microscopic 'signature' of strain within glacial sediments revealed using X-ray computed microtomography. *Quaternary Science Reviews* **30**: 3501–3532 [DOI: 10.1016/j.quascirev.2011.05.016].

Thomas GSP, Chiverrell RC. 2007. Structural and depositional evidence for repeated ice-marginal oscillation along the eastern margin of the Late Devensian Irish Sea Ice Stream. *Quaternary Science Reviews* **26**: 2375–2405.

Thomsen KJ, Murray AS, Bøtter-Jensen L. 2005. Sources of variability in OSL dose measurements using single grains of quartz. *Radiation Measurements* **39**: 47–61 [DOI: 10.1016/j.radmeas.2004.01.039].

van der Meer JJM. 1993. Microscopic evidence of subglacial deformation. *Quaternary Science Reviews* **12**: 553–587 [DOI: 10.1016/0277-3791(93)90069-X].

van der Meer JJM, Menzies J. 2011. The micromorphology of unconsolidated sediments. *Sedimentary Geology* **238**: 213–232 [DOI: 10.1016/j.sedgeo.2011.04.013].

Wintle AG. 1981. Thermoluminescence dating of Late Devensian loesses in southern England. *Nature* **289**: 479–480 [DOI: 10.1038/289479a0].

Xu S, Dougans AB, Freemand SPHT, Schnabel C, Wilcken KM. 2010. Improved ^{10}Be and ^{26}Al-AMS with a 5 MV spectrometer. Nuclear Instruments and Methods in Physics Research Section B: Beam Interactions with Materials and Atoms, 268, 736–738.

Young NE, Schaefer JM, Briner JP *et al.* 2013. A ^{10}Be production-rate calibration for the Arctic. *Journal of Quaternary Science* **28**: 515–526 [DOI: 10.1002/jqs.2642].

